CrossMark

Effects of hydrothermal treatment coupled with mechanical expression on combustion performance of Loy Yang lignite

Xiangchun Liu[1] · Tsuyoshi Hirajima[1,2] · Moriyasu Nonaka[1] · Keiko Sasaki[1]

Abstract The combustion characteristics and kinetics of hydrothermal treatment (HT) without addition of extra water and of HT coupled with mechanical expression (HT–ME) were investigated using thermogravimetric analysis at various heating rates. The relationships between various physicochemical properties, i.e., amounts of volatile matter and fixed carbon, specific surface area, and pore volume, and combustion performance were also investigated. The activation energy was calculated using the Kissinger–Akahira–Sunose isoconversional method. The results showed that for samples treated using HT and HT–ME, the ignition temperatures and temperatures at which the mass loss rates were at maximum, mainly because of char combustion, were significantly higher than those for raw lignite. They increased slightly with increasing processing temperature, suggesting that HT and HT–ME decrease the reactivity of Loy Yang lignite. The maximum combustion rates of the treated samples were higher than those of raw lignite and the values for the HT and HT–ME samples differed slightly from each other. The higher maximum combustion rates indicate that HT and HT–ME modify the combustion intensity of Loy Yang lignite. Furthermore, the combustion of raw lignite can be described by multistep kinetics, whereas single rate-limiting step kinetics can be used to describe the kinetics of the other samples. Average activation energies of samples treated using HT and HT–ME at 200 °C reached the maximum values.

Keywords Lignite · Thermogravimetric analysis · Combustion characteristics · Kinetics

Introduction

The use of low-rank coal is gradually becoming as important as that of high-rank coal because of the continuing increase in global energy demands, the decrease in high-rank coal reserves, and the wide availability of low-rank coal, which is estimated to represent 45 % of the world's coal reserves [1, 2]. Lignite is a typical low-rank coal, but its use is problematic because of its high tendency to undergo spontaneous combustion, its strong thermal reactivity, and high costs of transportation and storage because of its high water content. Lignite is therefore primarily used for electricity generation at power stations located at or near a mine. These problems arise because lignite contains abundant oxygen-containing functional groups and is highly porous [3–5]. Dewatering can partly solve these problems; however, for them to be completely solved, decomposition of oxygen-containing functional groups and collapse or blocking of pores during dewatering are necessary.

Many techniques for drying lignite have been developed. These can be grouped into two categories: evaporative and non-evaporative drying techniques [5]. Because

✉ Tsuyoshi Hirajima
hirajima@mine.kyushu-u.ac.jp

Xiangchun Liu
lxc625809204@163.com

[1] Department of Earth Resources Engineering, Faculty of Engineering, Kyushu University, 744 Motooka, Nishiku, Fukuoka 819-0395, Japan

[2] Research and Education Center of Carbon Resources, Kyushu University, 6-1 Kasuga-koen, Kasuga, Fukuoka 816-8580, Japan

the evaporative latent heat of water removed from low-rank coal is used in evaporative drying techniques, these drying techniques are not efficient. Non-evaporative techniques, such as mechanical and hydrothermal dewatering, have been developed to avoid the disadvantages of evaporative drying techniques. A more efficient non-evaporative technique, namely mechanical thermal dewatering, which is based on a combination of mechanical and hydrothermal techniques, has been developed [6]. The use of mechanical expression (ME) with heating during mechanical thermal dewatering is important for improving dewatering. This gives a highly consolidated solid product with collapse of pores and destruction of the colloidal structure, which can reduce the amount of readsorbed water and the reactivity of the solid product [1, 5]. The consolidated product can be easily handled and transported, with reduced environmental contamination. Pure ME dewatering is not suitable for technical applications because a high pressure should be maintained for at least 20 min [5]. In addition, non-evaporative drying changes the physicochemical properties of lignite, which can lead to changes in the combustion performance.

The combustion performance of lignite for use in industrial pulverized coal furnaces can be investigated using thermogravimetric (TG) analysis. TG analysis is an effective and simple technique [7–14]. It provides a rapid quantitative method for examining the overall combustion process and estimating the effective kinetic parameters; these are useful in engineering design and economic assessment. The ignition temperature (T_i), peak temperature (T_p), burnout temperature, and maximum combustion rate (MCR) are generally used to characterize combustion [7–16]. The activation energy (E), which is associated with the energy barrier, the pre-exponential factor (A), which is related to the vibrational frequency of the activated complex, and the dependence on the extent of conversion (α) by the reaction model [$f(\alpha)$], which is regarded as the reaction mechanism, are used to analyze the combustion kinetics [7–16]. Many studies of the combustion performance of lignite have been performed using TG analysis. In early studies, the combustion performance of lignite alone was studied [10–13]. Recently, researchers have focused on co-combustion of lignite and other substances such as coal gangue, sewage sludge, and chemical wastewater [14–16]. The combustion performance depends greatly on a number of factors such as the operating conditions (e.g., heating rate, reaction atmosphere, sample size, and water content of the sample) and physicochemical properties [e.g., specific surface area (SSA), pore volume, and amounts of volatile matter and char]. Different operating conditions can give different combustion characteristics and kinetic parameters. However, under the same conditions, TG analysis is a valuable tool for investigating changes in the combustion characteristics and kinetic parameters, which are useful for evaluating the combustion performance [7].

In this study, instead of conventional hydrothermal treatment (HT), HT without addition of extra water was performed; this reduces the amounts of wastewater and energy consumption. Solid samples obtained using HT were also treated using ME (HT–ME) at 110 °C under atmospheric conditions. Few studies have considered how the changes in the physicochemical properties caused by HT and HT–ME influence the combustion performance. In this work, TG analysis was used to investigate changes in the combustion performances of samples treated using HT and HT–ME with changes in the physicochemical properties, namely the SSA, pore volume, and amounts of volatile matter and fixed carbon. Non-isothermal thermogravimetry was performed at four different heating rates, and the Kissinger–Akahira–Sunose (KAS) isoconversional method was used to calculate the kinetic parameters.

Experimental

Sample

An Australian lignite (Loy Yang, LY) was used as the coal sample and was ground to pass through an 840-μm sieve. The proximate and ultimate analyses are listed in Table 1.

Hydrothermal treatment

Details of the HT apparatus and experimental procedure have been reported previously [17, 18]. Briefly, raw lignite (about 6 g) was placed in a steel filter ($\phi = 60$ μm), and three of the steel filters were fixed in the middle of the cylinder of a 0.5-L batch-type reactor (MA22, Taiatsu Techno, Japan) equipped with an automatic temperature controller with a maximum temperature of 400 °C and a maximum pressure of 30 MPa (Fig. 1). N_2 gas was flushed through the sealed system to remove air. The reactor was then pressurized with N_2 gas to 1.5 MPa at room temperature. A series of HTs were performed at different temperatures (150, 200, and 250 °C) for 40 min at an average heating rate of ca. 5 °C min^{-1}. The reactor was cooled to room temperature, and the solid products were collected. The samples are denoted by HT150, HT200, and HT250 for HT temperatures of 150, 200, and 250 °C, respectively. Curves of the saturated steam pressure against temperature and of the pressure in the closed reactor against temperature were plotted (Fig. 2) and used to check whether the HT condition (i.e., the pressure in the reactor is at least slightly higher than the saturated steam pressure) could be maintained without adding extra water. The results showed that the HT condition was maintained.

Table 1 Proximate and ultimate analyses of raw lignite

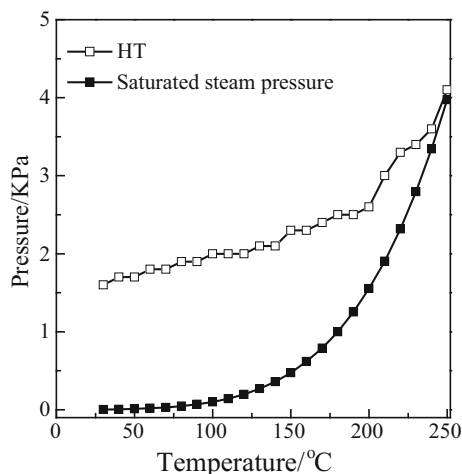| Lignite	Proximate analysis/mass%				Ultimate analysis[a]/mass%, daf				Mass%, daf
	M_{ar}	A_d	V_{daf}	FC_{daf}	C	H	N	(O + S)/diff.	S_{total}^{b}
LY	57.5	0.7	51.3	48.7	64.8	4.9	0.6	29.7	0.3

ar as received basis, *daf* dry ash-free basis, *d* dry basis, *M* moisture, *A* ash, *V* volatile matter, *FC* fixed carbon

[a] Conducted using a CHN elemental analyzer (CORDER MT-6, Yanaco, Japan)
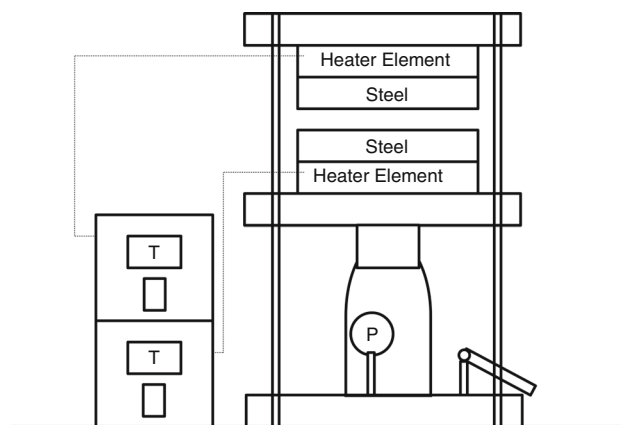
[b] Measured by Eschka method
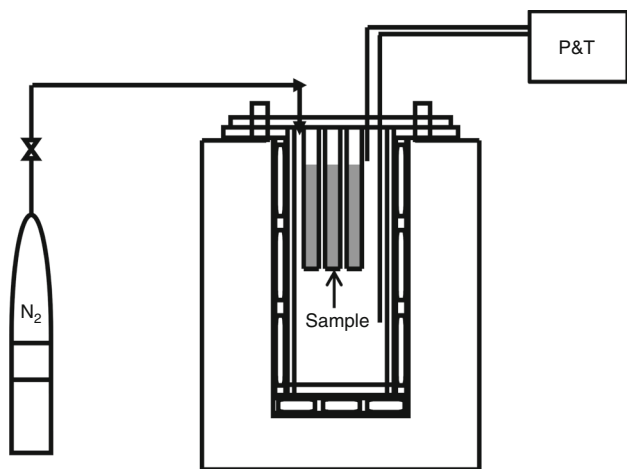
Fig. 1 Schematic of HT batch-type reactor

Fig. 3 Schematic of mechanical expression equipment

Fig. 2 Curves of the saturated steam pressure against temperature and of the pressure in the closed reactor against temperature during HT process in this paper

Hydrothermal treatment coupled with mechanical expression

The HT solid products and raw lignite were placed in fixed regions of filter papers to ensure that the sizes of the samples treated using ME were the same. A small pressing machine (AH-2003, ASONE, Japan; Fig. 3) was heated to a prescribed temperature (110 °C). When the desired temperature was reached, the machine was used to apply a mechanical pressure of 6 MPa to the samples for 20 min under atmospheric conditions. The treated samples were denoted by HT150–ME, HT200–ME, and HT250–ME, and raw lignite directly treated by ME was denoted by RL–ME.

Calculation of kinetic parameters

The isoconversional method does not depend on prior assumptions or any particular form of the reaction model. It has been proved to be effective and is highly recommended for kinetic analysis by the International Confederation for Thermal Analysis and Calorimetry (ICTAC) Kinetics Committee [10]. The principle of the isoconversional method is that the reaction rate at a constant α is a function of temperature only. The KAS method is one of the most popular isoconversional methods for determining thermal kinetic parameters because it is computationally simple and its accuracy is adequate for most practical purposes [10, 19]. The KAS equation can be obtained from the literature [19]. Briefly, the Arrhenius law is

$$\frac{d\alpha}{dt} = Ae^{\left(\frac{-E}{RT}\right)} f(\alpha),\tag{1}$$

where $\alpha = (m_0 - m_i)/(m_0 - m_\infty)$ is the extent of conversion (m_0, m_∞, and m_i are the initial, final, and instantaneous mass, respectively); t is the combustion time (s); A is the pre-exponential factor; E is the activation energy (J mol^{-1} K^{-1}); R is the gas constant (J mol^{-1} K^{-1}); and T is the temperature (K). The heating rate (°C min^{-1}) is

$$\beta = dT/dt.\tag{2}$$

Combining Eqs. (1) and (2) give

$$\frac{d\alpha}{f(\alpha)} = \frac{A}{\beta} \cdot e^{\left(\frac{-E}{RT}\right)} dT.\tag{3}$$

Integrating Eq. (3) gives

$$\int_0^\alpha \frac{d\alpha}{f(\alpha)} = \frac{A}{\beta} \int_0^T e^{\left(-\frac{E}{RT}\right)} dT = \frac{AE}{\beta R} \int_y^\infty \frac{e^{(-y)}}{y^2} dy,\tag{4}$$

where

$$y = E/RT,\tag{5}$$

$$\int_y^\infty \frac{e^{(-y)}}{y^2} dy = \frac{e^{(-y)}}{y^2} \left(1 + \frac{2!}{y} + \frac{3!}{y^2} + \frac{4!}{y^3} + \cdots\right).\tag{6}$$

Truncating the series to the first-order approximation gives

$$\int_y^\infty \frac{e^{(-y)}}{y^2} dy \approx \frac{e^{(-y)}}{y^2}.\tag{7}$$

The KAS equation can therefore be obtained by taking the logarithm of Eq. (4) and using Eq. (7):

$$\ln \frac{\beta}{T^2} = -\frac{E}{RT} + ln \frac{AR}{E \int_0^\alpha d\alpha/f(\alpha)}.\tag{8}$$

The ICTAC Kinetics Committee recommends performing a series of three to five runs for calculation of reliable kinetic parameters [10]. The following form of the KAS equation is therefore frequently used:

$$\ln \frac{\beta_i}{T_{\alpha,i}^2} = \frac{E_\alpha}{RT_{\alpha,i}} + ln \frac{AR}{E \int_0^\alpha d\alpha/f(\alpha)},\tag{9}$$

where i denotes various heating rates. $T_{\alpha,i}$ is the temperature at a given α at the ith heating rate. The second term on the right-hand side of Eq. (9) is a constant at a given α for different heating rates, based on isoconversional methods [19]. The E at each given α value (E_α) is determined from the slope of a plot of $\ln(\beta_i/T_{\alpha,i}^2)$ against $1/T_{\alpha,i}$ at heating rates of 2, 4, 8, and 16 °C min^{-1}. An example is shown in Fig. 4. Note that the experimentally determined E is appropriate to call an "effective", "apparent", "empirical," or "global" E to stress that it can deviate from the intrinsic value of a specific individual step [10].

Characterization

The lignite water content was measured based on the fractional mass release during heating in an oven (WFO-50, Eyela, Japan) at 105 °C for 6 h. The ash content was calculated as the mass of waste remaining after treatment of the lignite in a furnace (TFM-2200, Eyela) at 815 °C for 2.5 h. The volatile matter was calculated as the mass release observed on heating in the furnace at 900 °C for 7 min. The SSAs, macro- and mesopore size distributions, and micropore size distributions were calculated using the Brunauer–Emmett–Teller, Barrett–Joyner–Halenda, and Horvath–Kawazoe equations, respectively, based on the adsorption isotherms, which were measured by N_2 gas adsorption at 77 K using a high-precision SSA and pore size distribution analyzer (BEL-Max, BEL, Japan). For the N_2 gas adsorption experiments, pre-treatment under vacuum at 110 °C for 15 h was performed to remove adsorbed gases. TG tests were performed by placing the sample (3 mg) in a platinum crucible on a thermal analyzer (2000SA, Bruker, USA). The samples were heated from room temperature to 600 °C at a series of different heating rates (2, 4, 8, and 16 °C min^{-1}) under an air flow rate of 25 mL min^{-1}. The characterizations were repeated at least twice. The morphologies of the samples before and after treatment were observed using scanning electron microscopy (SEM; VE-9800, Keyence, Japan).

Results and discussion

Effects of HT and HT–ME on pore size distribution

The pore structure has a significant effect on the combustion performance of lignite; the pore size distributions of all the samples are shown in Fig. 5. According to the International Union of Pure and Applied Chemistry classification, the diameter ranges of macropores, mesopores, and micropores are >50 nm, 2–50 nm, and <2 nm, respectively. The pore size range was divided into three regions, i.e., macro-, meso-, and micropore regions, to aid analysis of the pore size distribution data (Fig. 5).

Figure 5a, b shows that the porosities of the macro- and micropores of HT150 were lower than those of raw lignite, whereas the mesopore porosity was slightly higher than that of raw lignite. The porosities of the macro-, meso-, and micropores of HT200 were higher than those of HT150, which were significantly higher than those of HT250. The porosity changes at temperatures below 200 °C can be understood in terms of competition between development
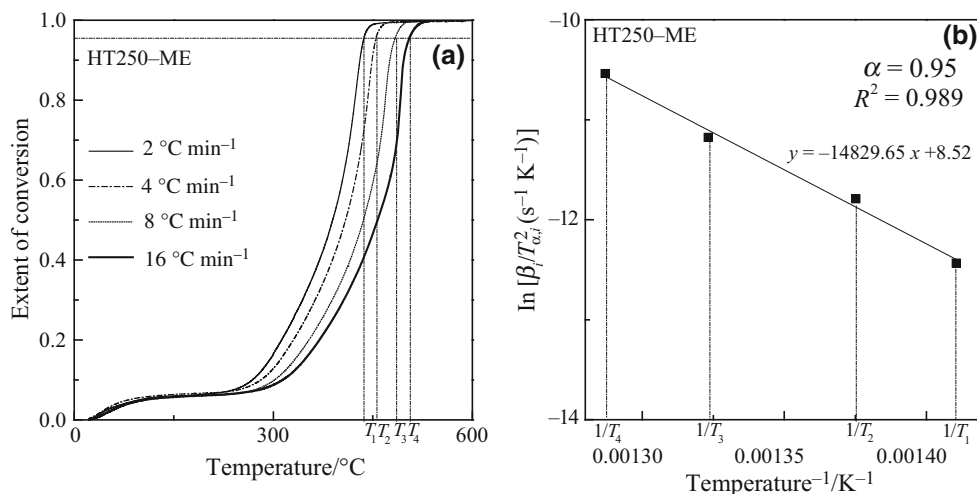
Fig. 4 Example of kinetics calculation by the KAS method. **a** Relationship between temperature and α of HT250–ME, **b** curve of fitting to kinetic model by the KAS method to α = 0.95 corresponding to the combustion of HT250–ME at β = 2, 4, 8, and 16 °C min^{-1}
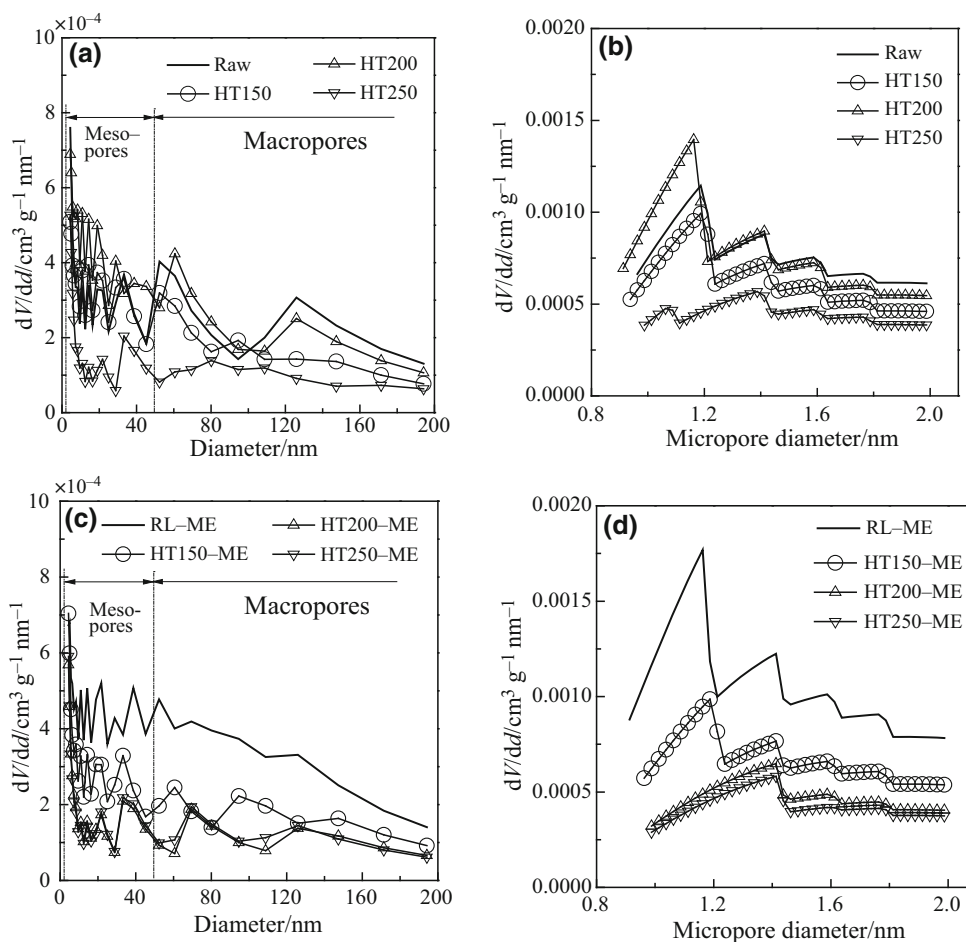
Fig. 5 Effects of HT and HT–ME on pore size distribution

and collapse of pores. Pores develop because of opening and cross-linking of closed pores, as well as removal of organic matter during dewatering. The collapse of pores is caused by increases in the diameters of old pores and shrinkage forces caused by drying. Above 200 °C, not only pore collapse but also disintegration of the macromolecular

structure as a result of significant thermal decomposition occurs [17]. As a result of these two factors, the porosity of HT250 was markedly lower than that of HT200.

The porosities of the macro-, meso-, and micropores of the treated samples (Fig. 5c, d) continuously decreased from RL–ME to HT250–ME. This is the result of the effects of compression during ME treatment and pore collapse. Note that the porosities of the macro-, meso-, and micropores of RL–ME were higher than those of raw lignite. The water content of RL–ME was low (Table 2). The release of water from closed and blind pores of RL–ME led to opening and linking of these pores [20]. As a result, the pore volume increased. Furthermore, the colloidal properties of raw lignite cannot be destroyed without HT. The effect of compression during ME treatment on the porosity, which can decrease the pore volume, was therefore negligible without HT. The differences among the surface morphologies were examined using SEM; images of some representative samples are shown in Fig. 6. Figures 5 and 6 show that the number of pore networks in RL–ME was higher than that in raw lignite because of pore development, whereas the numbers of pore networks in HT250 and HT150–ME were lower as a result of collapse, disintegration, and compression of pores.

Effects of HT and HT–ME on lignite combustion characteristics

A large sample mass causes heat accumulation in the sample; therefore, a small amount of sample is better for TG experiments. To obtain high-quality experimental data, a series of experiments using 2, 3, and 5 mg of lignite were performed to determine the most suitable sample mass; the results are shown in Fig. 7. The derivative TG (DTG) curve for 2 mg of sample contained too much noise. The 3 mg sample gave the best result. Therefore, this amount was used for subsequent experiments.
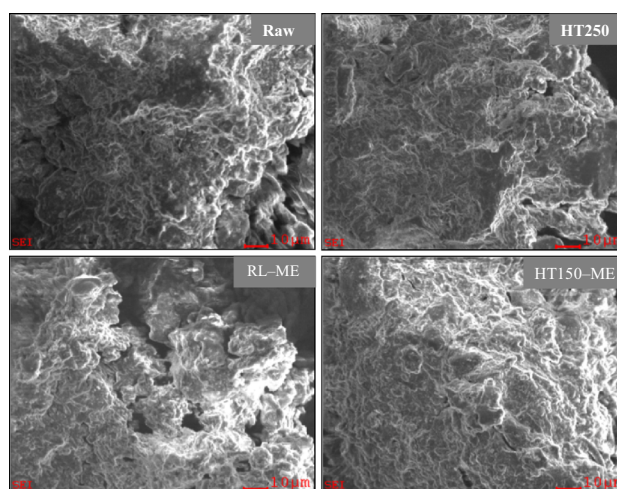

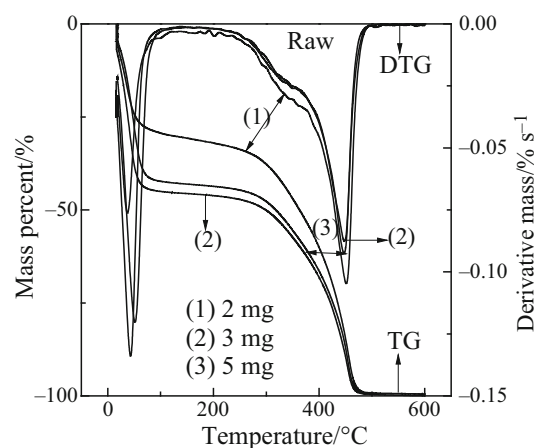Fig. 6 Typical samples under SEM observation

Fig. 7 Effect of sample mass on TG and DTG curves

The combustion characteristics of lignite are usually investigated by TG analysis. The plot of mass against temperature (TG curve) clearly shows a gradual process of mass loss. The mass loss against temperature (DTG curve)

Table 2 Effect of HT and HT–ME on combustion characteristic parameters and some physicochemical properties of all of the samples

Sample	T_i/°C	TP_2/°C	MCR/% s^{-1}	SSA/m^2 g^{-1}	Total volume of macro- and mesopore/cm^3 g^{-1}	M/[(g g^{-1}) 100 %][a]	A/[(g g^{-1}) 100 %][a]	V/[(g g^{-1}) 100 %][a]	FC/[(g g^{-1}) 100 %][a]
Raw	381	449	0.09	3.6 ± 0.2	0.023 ± 0.001	57.47 ± 0.14	0.31 ± 0.02	21.67 ± 0.09	20.54 ± 0.03
HT150	405	460	0.15	3.0 ± 0.5	0.018 ± 0.001	15.85 ± 4.11	0.60 ± 0.01	42.99 ± 0.03	40.57 ± 0.02
HT200	409	463	0.15	3.7 ± 0.3	0.024 ± 0.001	7.60 ± 0.84	0.40 ± 0.05	45.75 ± 0.56	46.24 ± 0.56
HT250	415	463	0.17	2.2 ± 0.3	0.010 ± 0.004	5.87 ± 0.71	0.68 ± 0.02	45.85 ± 0.62	47.61 ± 0.59
RL–ME	404	459	0.19	4.9 ± 0.1	0.032 ± 0.002	4.25 ± 0.16	0.80 ± 0.01	47.97 ± 0.09	46.98 ± 0.09
HT150–ME	406	456	0.18	3.2 ± 0.1	0.018 ± 0.000	3.38 ± 0.18	0.68 ± 0.01	48.57 ± 0.16	47.37 ± 0.15
HT200–ME	410	463	0.17	2.3 ± 0.2	0.012 ± 0.001	1.67 ± 0.39	0.60 ± 0.02	48.13 ± 0.38	49.59 ± 0.39
HT250–ME	419	463	0.18	2.2 ± 0.2	0.012 ± 0.000	0.92 ± 0.12	0.74 ± 0.02	48.46 ± 0.11	49.87 ± 0.08

[a] On the basis of the total mass of sample

plot provides the combustion rate. In the heat released against temperature plot [differential thermal analysis (DTA) curve], either exothermic or endothermic processes can be observed [21]. As mentioned in the Introduction, TG analysis under the same conditions is a valuable tool for comparing combustion characteristics. In this study, a heating rate of 8 °C min^{-1} was used to investigate changes in the combustion characteristics. Figures S1 and S2 show TG, DTG, and DTA curves of the samples treated using HT and HT–ME, respectively. The curves were divided into three regions, based on the approximate start and end points of the DTA curves. An example of this method is shown in Fig. 8. The first region ($T \leq 150$ °C) mainly represents removal of water, and the second region ($150 < T \leq 370$ °C) represents devolatilization and combustion of volatile matter. In the third region ($370 < T \leq 490$ °C), burning of solid char formed by decomposition, polycondensation, solidification, and shrinkage of fixed carbon occurs and continues until the ash level is reached. The higher the fixed carbon content, the higher the obtained char content will be. In this study, attention was primarily focused on regions 2 and 3.

Ignition of lignite can be described as a process of achieving a continual reaction between an oxidizer and lignite, which affects the flame stability and extinction [7]. The combustibility of coal can be expressed in terms of T_i, T_p, and the MCR [7–16]. Several methods can be used to determine T_i [11, 19, 21–24], and the T_i values differ slightly depending on the method used. However, T_i values can be quantitatively compared when the same method is used. The definition of T_i in this study is taken from the literature [22]. In brief, as shown in Fig. 8, a vertical line is first made through the DTG peak point A, to meet the TG curve at point B. The tangent to the TG curve through point
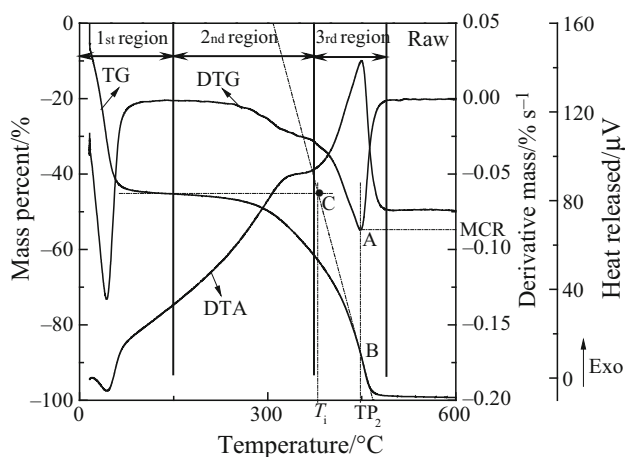
B and the initial baseline of the TG curve meet at point C. T_i is the corresponding temperature at point C. The two DTA peaks show that ignition of volatile matter and char occurred at different temperatures. T_i achieved by ignition of volatile matter is commonly referred to as "false ignition" because the coal will not necessarily burn out unless the temperature is further increased to ignite the char [11]. In the present work, T_i was in region 3, which corresponded to char ignition. The temperature of peak 2 (TP$_2$) is defined as the point at which the rate of mass loss is maximum (DTG curve), mainly because of char combustion. The rate of maximum mass loss at TP$_2$ is called the MCR (Fig. 8). These combustion parameters and some physicochemical properties of all the samples are listed in Table 2. It should be noted that the pore structure of lignite consisted mainly of macro- and mesopores [25]. The N_2 gas adsorption–desorption isotherms confirmed that the number of micropores in the lignite was negligible (Figs. S3 and S4). The total volume of macro- and mesopores (TV) without the micropore volume is given in Table 2.

T_i depends on the amount and boiling point of volatile matter, the char content, and the speed of heat released by volatile matter and char combustion. The combustion of volatile matter plays a preheating role in char combustion. Char acts as a diffusion barrier for combustible components (e.g., oxygen and char) and a thermal insulation barrier [8]. The MCR is mainly determined by the char content, the accessibility of an oxidizer to the active sites in the sample, and the SSA for oxidation [26]. These factors, which control T_i and the MCR, influence TP$_2$.

Table 2 shows that the T_i, TP$_2$, and MCR values of raw lignite and the samples treated using HT and HT–ME varied greatly, suggesting that HT and HT–ME affected the combustion characteristics of lignite. T_i and TP$_2$ are inversely proportional to the reactivity of lignite, i.e., the lower T_i (or TP$_2$), the more reactive the coal is [27]. The T_i and TP$_2$ values for the samples treated using HT and HT–ME were significantly higher than those for raw lignite, and they increased slightly with increasing processing temperature. This is because the raw lignite contains a relatively high amount of low-boiling-point volatile matter, which is released from the lignite at relative low temperatures, and a small amount of char (Table 2). After HT, the content of high-boiling-point volatile matter, which is removed at relative high temperatures, increased and the char in the treated samples led to increase in the T_i and TP$_2$ values. For the samples treated using HT–ME, although the changes in their volatile matter contents were negligible, the char content increased slightly, i.e., the same phenomenon were observed as for the samples treated using HT and HT–ME. For the samples treated using HT and HT–ME, the amounts of high-boiling-point volatile matter and char increased slightly with increasing processing temperature; this is the

Fig. 8 TG, DTG, and DTA curves of raw lignite at $\beta = 8$ °C min^{-1}. T_i as ignition temperature, TP$_2$ as the peak temperature of the second region, MCR as the maximum combustion rate

reason for the slight increases in the T_i and TP_2 values. In summary, the changes in T_i and TP_2 indicate that HT and HT–ME can significantly decrease the reactivity of raw lignite and the reactivities of the treated samples gradually decrease as a result of these two processes.

A comparison of the MCRs shows that the values for the samples treated using HT and HT–ME were higher than those for raw lignite, and the changes in the MCRs of the treated samples with increasing temperature were negligible. A higher char content and larger SSA can provide more active sites, and increasing the TV can improve accessibility for the oxidizer. For RL–ME and HT200, the synergistic effect of the increases in char content, SSA, and TV relative to those of raw lignite resulted in higher MCRs compared with that of raw lignite. For the other samples, the increases in the MCRs can be attributed to competition between the increases in char contents and the decreases in the SSAs and TVs. In addition, the increased MCRs show that the combustion intensities of the samples treated using HT and HT–ME can be improved.

The T_i and MCR values of the samples treated using HT–ME were slightly higher than those of the corresponding samples treated using HT. The TP_2 values of the samples treated using HT–ME were similar to those of the corresponding samples treated using HT. These results suggest that HT–ME slightly changed the reactivity and combustion intensity of LY lignite compared with those obtained using HT.

Effects of HT and HT–ME on lignite combustion kinetics

Lignite combustion is a complicated process that generally involves removal of water, release and combustion of volatile matter, and char burning. The total mass loss in TG experiments is therefore the result of the combined changes in the amounts of water, volatile matter, and char. The ICTAC Kinetics Committee recommends that an α interval not greater than 0.05 should be used in the determination of E_α. An α interval of 0.05 was chosen in this work. E_α was calculated for α values of 0.20–0.95 because most solid-state reactions are not stable in the initial and final periods [19]. The E_α values calculated from plot slopes using the KAS method had high correlation coefficients (R^2), as listed in Tables 3 and 4. For raw lignite, the initial α value was 0.6 because at $\alpha < 0.6$ removal of water occurs, which was not considered in this study.

Lignite combustion involves several steps. The changes in E_α with α, determined using an isoconversional method, show whether the sample combustion obeys multistep kinetics or single rate-limiting step kinetics, in which the mechanism involves several steps but one of them dominates the overall kinetics [10]. For raw lignite, the E_α value

varied significantly with changes in α and the difference between the maximum and minimum values was 70.5 kJ/mol, which was more than 20–30 % of the average activation energy (E_a). This suggests that the raw lignite combustion kinetics was multistep [10]. However, for the other samples, the E_α values did not vary significantly with α, indicating that these processes can be described by single rate-limiting step kinetics.

Changes in E_α with α reflect general trends in the combustion process. The E_α values generally increased with increasing α. This is because combustion of low-boiling-point volatile matter changes to combustion of high-boiling-point volatile matter, where E_α gradually increases, and then changes to char burning with increasing α. The E of volatile matter combustion is lower than that of char [28, 29]. This is consistent with the findings of Vyazovkin et al. [10], who reported that the E_α of fossil fuels increases with increasing α because the residual material becomes increasingly refractory. Furthermore, the change trends in the E_α values with α for HT200–ME and HT250–ME were smaller than those for the other samples. The changes in E_α with α reflect a change from combustion of volatile matter to char combustion. More low-boiling-point volatile matter is released from HT200–ME and HT250–ME, leading to an increase in E at low α values. Therefore, the differences between the E_α values of the volatile matter remaining in the samples and char decreased. As a result, the smaller change trends were found. The E_α of HT200–ME was higher than that of HT250–ME; this can be explained by the effects of increased diffusion and formation of new lower E char. A more detailed analysis of this point is provided later.

The E_a values for the samples treated using HT and HT–ME (108.6–113.3 and 108.4–120.9 kJ/mol, respectively) were higher than that for raw lignite (104.5 kJ/mol), indicating that HT and HT–ME can lower the overall reactivity in LY lignite combustion. For the samples treated using HT and those treated using HT–ME, the E_a values increased slightly and reached the maximum values for HT200 and HT200–ME. This can be attributed to increases in the amounts of char carbon and high-boiling-point volatile matter (Table 2), leading to increased E_a values. The E_a values decreased for HT250 and HT250–ME. As we previously reported [30], the carboxyl group contents of HT200, HT250, HT200–ME, and HT250–ME were 1.45, 0.78, 1.40, and 0.88 (mmol/g, d), respectively. The char contents of HT250 and HT250–ME, respectively, were higher than those of HT200 and HT200–ME, respectively (Table 2). This suggests that more oxidizer from the external environment was required for HT250 and HT250–ME than for HT200 and HT200–ME. Furthermore, the TV of HT250 decreased significantly relative to that of HT200 and the TVs of HT250 and HT250–ME changed

Table 3 Combustion kinetic parameters of samples treated by HT calculated by KAS method

Raw			HT150		HT200		HT250	
α	$E/\text{kJ mol}^{-1}$	R^2	$E/\text{kJ mol}^{-1}$	R^2	$E/\text{kJ mol}^{-1}$	R^2	$E/\text{kJ mol}^{-1}$	R^2
0.20			94.4 ± 3.5	0.967	101.2 ± 4.0	0.993	96.7 ± 9.3	0.985
0.25			97.4 ± 4.2	0.985	101.7 ± 1.3	0.990	97.9 ± 8.7	0.988
0.30			98.3 ± 3.7	0.993	102.4 ± 1.1	0.987	100.6 ± 8.3	0.988
0.35			100.8 ± 3.1	0.995	104.6 ± 0.5	0.986	103.6 ± 7.6	0.989
0.40			104.2 ± 2.9	0.996	107.9 ± 0.1	0.986	106.2 ± 6.6	0.989
0.45			107.5 ± 2.9	0.997	111.0 ± 0.6	0.988	108.3 ± 6.1	0.991
0.50			110.8 ± 3.1	0.997	112.9 ± 1.2	0.990	110.1 ± 5.3	0.991
0.55			112.4 ± 3.4	0.996	114.7 ± 1.5	0.992	111.2 ± 4.8	0.992
0.60	63.8 ± 1.3	0.973	113.2 ± 3.4	0.994	115.2 ± 2.1	0.994	111.2 ± 4.2	0.992
0.65	75.2 ± 1.1	0.977	113.7 ± 3.1	0.995	115.7 ± 2.0	0.995	111.9 ± 3.9	0.993
0.70	87.5 ± 3.2	0.980	114.7 ± 2.2	0.995	117.2 ± 2.0	0.996	113.0 ± 3.9	0.994
0.75	102.5 ± 6.0	0.984	116.8 ± 1.7	0.996	118.9 ± 2.2	0.996	114.7 ± 3.7	0.994
0.80	116.7 ± 8.7	0.988	119.3 ± 2.2	0.996	121.7 ± 2.6	0.996	115.6 ± 4.3	0.993
0.85	125.5 ± 10.6	0.990	120.3 ± 3.1	0.995	123.5 ± 3.9	0.995	114.6 ± 5.1	0.990
0.90	130.5 ± 10.8	0.991	119.0 ± 4.1	0.991	123.7 ± 5.8	0.994	112.3 ± 5.1	0.988
0.95	134.3 ± 12.1	0.991	116.1 ± 3.9	0.985	121.3 ± 5.4	0.995	110.0 ± 4.6	0.990
$(E_a)^a$	104.5 ± 6.1		109.9 ± 3.1		113.3 ± 1.4		108.6 ± 5.7	

[a] As average activation energy

Table 4 Combustion kinetic parameters of samples treated by HT–ME calculated by KAS method

RL–ME			HT150–ME		HT200–ME		HT250–ME	
α	$E/\text{kJ mol}^{-1}$	R^2	$E/\text{kJ mol}^{-1}$	R^2	$E/\text{kJ mol}^{-1}$	R^2	$E/\text{kJ mol}^{-1}$	R^2
0.20	114.4 ± 13.3	0.957	98.8 ± 4.9	0.972	121.5 ± 4.0	0.999	103.2 ± 2.7	0.987
0.25	91.1 ± 24.2	0.941	99.8 ± 2.4	0.976	117.5 ± 5.6	0.999	102.2 ± 1.0	0.988
0.30	105.7 ± 2.4	0.991	100.9 ± 0.7	0.977	117.0 ± 6.4	0.999	102.3 ± 0.2	0.989
0.35	104.6 ± 1.2	0.993	103.7 ± 1.0	0.979	118.3 ± 6.6	0.999	103.9 ± 0.1	0.990
0.40	105.5 ± 0.0	0.994	107.3 ± 2.0	0.981	119.7 ± 7.1	0.999	105.1 ± 0.6	0.992
0.45	107.3 ± 1.0	0.996	110.5 ± 3.0	0.983	121.2 ± 7.6	0.999	106.7 ± 1.4	0.994
0.50	109.1 ± 1.8	0.997	113.0 ± 3.9	0.984	121.8 ± 7.7	0.999	107.4 ± 1.4	0.995
0.55	110.3 ± 2.0	0.997	115.0 ± 4.3	0.985	120.9 ± 6.7	0.999	107.4 ± 1.6	0.996
0.60	110.4 ± 2.5	0.997	115.4 ± 4.6	0.985	119.4 ± 5.9	0.998	107.2 ± 1.7	0.996
0.65	109.5 ± 2.7	0.996	115.8 ± 4.5	0.986	119.1 ± 5.3	0.998	108.0 ± 1.7	0.996
0.70	108.0 ± 0.8	0.994	116.2 ± 4.3	0.986	120.5 ± 4.5	0.998	109.9 ± 2.3	0.996
0.75	108.8 ± 0.9	0.996	118.5 ± 5.0	0.988	119.7 ± 8.4	0.995	112.1 ± 3.0	0.996
0.80	111.3 ± 2.0	0.997	122.6 ± 5.6	0.989	124.4 ± 7.6	0.998	114.2 ± 5.3	0.996
0.85	116.7 ± 1.8	0.998	127.0 ± 6.6	0.990	125.6 ± 9.1	0.998	115.5 ± 8.4	0.994
0.90	123.7 ± 1.8	0.998	129.8 ± 8.0	0.989	124.8 ± 10.6	0.998	115.7 ± 10.2	0.992
0.95	128.4 ± 7.6	0.998	128.3 ± 9.7	0.984	123.4 ± 10.3	0.998	114.4 ± 8.9	0.991
E_a	110.3 ± 1.6		113.9 ± 3.4		120.9 ± 7.1		108.4 ± 2.7	

slightly (Table 2). These factors increased the effect of diffusion on E_a. The E value for chemical control, i.e., control by a chemical reaction, is higher than that for diffusion, which involves physical control. This perhaps is one reason for the phenomenon. On the other hand, as shown in our previous study [30], glucose and xylose were found in a liquid product obtained using HT because lignite is low-rank coal and contains plant materials. Iryani [31] found that in HT above 200 °C, 5-hydroxymethyl-furfural (5-HMF) and furfural are generated from the

decomposition of glucose and xylose, respectively. Further conversions of 5-HMF and furfural above 240 °C, e.g., 5-HMF polymerization, increase the amount of char [31]. Similarly, it is possible that some new lower E char was formed for HT250 and HT250–ME, which may be another reason for the decrease in E_a. In summary, HT can decrease the reactivity of LY lignite and ME can further slightly decrease the reactivity.

Conclusions

The T_i and TP$_2$ values for samples treated using HT and HT–ME were significantly higher than the corresponding values for raw lignite, and they increased slightly with increasing treatment temperature. This is because the amounts of high-boiling-point volatile matter and char in the treated samples are higher than those in raw lignite, leading to increases in the T_i and TP$_2$ values. The changes with increasing temperature in the amount and boiling point of volatile matter and the char content are small, resulting in only a slight increase in their T_i and TP$_2$ values. The MCRs of the treated samples were slightly higher than that of raw lignite, and the MCRs did not change significantly with increasing temperature. This may arise from the overall effects of differences among the char contents, SSAs, and TVs.

The combustion of raw lignite follows multistep kinetics, whereas the other samples follow single rate-limiting step kinetics. The E_a values of the treated samples were higher than that of raw lignite.

The T_i, MCR, and E_a values of the samples treated using HT–ME were slightly higher than those of the corresponding samples treated using HT. In summary, HT and HT–ME both decrease the reactivity and increase the combustion intensity of LY lignite, and the changes are slightly higher for HT–ME than for HT.

References

1. Karthikeyan M, Zhonghua W, Mujumdar AS. Low-rank coal drying technologies—current status and new developments. Drying Technol. 2009;27:403–15.
2. Yang XJ, Zhang C, Tan P, Yang T, Fang QY, Chen G. Properties of upgraded Shengli lignite and its behavior for gasification. Energy Fuels. 2014;28:264–74.
3. Man CH, Zhu X, Gao XZ, Che DF. Combustion and pollutant emission characteristics of lignite dried by low temperature air. Drying Technol. 2015;33:616–31.
4. Liu M, Yan JJ, Bai BF, Chong DT, Guo XK, Xiao F. Theoretical study and case analysis for a predried lignite-fired power system. Drying Technol. 2011;29:1219–29.
5. Li CZ. Advances in the science of Victorian brown coal. Amsterdam: Elsevier; 2004.
6. Liu M, Yan JJ, Wang JS, Chong DT, Liu JP. Thermodynamic analysis on a lignite-fired power system integrated with a steam dryer: investigation on energy supply system of the dryer. Drying Technol. 2015;33:1510–21.
7. Liu XC, Feng L, Song LL, Wang XH, Zhang Y. Effect of NaOH treatment on combustion performance of Xilinhaote lignite. Int J Min Sci Technol. 2014;24:51–5.
8. Yorulmaz SY, Atimtay AT. Investigation of combustion kinetics of treated and untreated waste wood samples with thermogravimetric analysis. Fuel Process Technol. 2009;90:939–46.
9. Schniewind AP. Concise encyclopedia of wood and wood based materials. 1st ed. Elmsford: Pergamon Press; 1989.
10. Vyazovkin S, Burnham AK, Criado JM, Pérez-Maqueda LA, Popescu C, Sbirrazzuoli N. ICTAC Kinetics Committee recommendations for performing kinetic computations on thermal analysis data. Thermochim Acta. 2011;520:1–19.
11. Ma S, Hill JO, Heng S. A thermal analysis study of the combustion characteristics of Victorian brown coals. J Therm Anal. 1989;35:1985–96.
12. Contreras ML, García-Frutos FJ, Bahillo A. Study of the thermal behaviour of coal/biomass blends during oxy-fuel combustion by thermogravimetric analysis. J Therm Anal. 2016;123:1643–55.
13. Tseng HP, Edgar TF. Identification of the combustion behaviour of lignite char between 350 and 900 °C. Fuel. 1984;63:385–93.
14. Zhang YY, Nakano J, Liu LL, Wang XD, Zhang ZT. Co-combustion and emission characteristics of coal gangue and low-quality coal. J Therm Anal. 2015;120:1883–92.
15. Vamvuka D, Sfakiotakis S, Saxioni S. Evaluation of urban wastes as promising co-fuels for energy production—A TG/MS study. Fuel. 2015;147:170–83.
16. Chen JB, Mu L, Cai JC, Yin HC, Song XG, Li AM. Thermal characteristics and kinetics of refining and chemicals wastewater, lignite and their blends during combustion. Energy Convers Manag. 2015;100:201–11.
17. Liu XC, Hirajima T, Nonaka M, Sasaki K. Investigation of the changes in hydrogen bonds during low temperature pyrolysis of lignite by diffuse reflectance FT-IR combined with forms of water. Ind Eng Chem Res. 2015;54:8971–8.
18. Mursito AT, Hirajima T, Sasaki K. Upgrading and dewatering of raw tropical peat by hydrothermal treatment. Fuel. 2010;89:635–41.
19. Wang CA, Du YB, Che DF. Reactivities of coals and synthetic model coal under oxy-fuel conditions. Thermochim Acta. 2013;553:8–15.
20. Liu JZ, Zhu JF, Cheng J, Zhou JH, Cen KF. Pore structure and fractal analysis of Ximeng lignite under microwave irradiation. Fuel. 2015;146:41–50.
21. Ren FM, Yue F, Gao M, Yu M. Combustion characteristics of coal and refuse from passenger trains. Waste Manag. 2010;30:1196–205.
22. Li XG, Ma BG, Liu X, Hu ZW, Wang XG. Thermogravimetric analysis of the cocombustion of the blends with high ash coal and waste tyres. Thermochim Acta. 2006;441:79–83.
23. Pranda P, Prandová K, Hlavacek V. Combustion of fly-ash carbon Part I. TG/DTA study of ignition temperature. Fuel Process Technol. 1999;61:211–21.
24. Liu XG, Li BQ, Miura K. Analysis of pyrolysis and gasification reactions of hydrothermally and supercritically upgraded low-rank coal by using a new distributed activation energy model. Fuel Process Technol. 2001;69:1–12.

25. Mahidin, Ogaki Y, Usui H, Okuma O. The advantages of vacuum-treatment in the thermal upgrading of low-rank coals on the improvement of dewatering and devolatilization. Fuel Process Technol. 2003;84:147–60.

26. Serageldin MA, Hai W. A thermogravimetric study of coal decomposition under ignition conditions. Thermochim Acta. 1990;171:193–206.

27. Cumming JW. Reactivity assessment of coals via a weighted mean activation energy. Fuel. 1984;63:1436–40.

28. Liu Z, Li WH, Zhang YS, Wang JW, Orndorff W, Pan WP. Influence of biomass on coal combustion based on thermogravimetry and Fourier transform infrared spectroscopy. J Therm Anal. 2015;122:1289–98.

29. Hakvoot G, Schouten JC, Valkenburg PJM. The determination of coal combustion kinetics with thermogravimetry. J Therm Anal. 1989;35:335–46.

30. Liu XC, Hirajima T, Nonaka M, Sasaki K. Hydrothermal treatment coupled with mechanical expression for Loy Yang lignite dewatering and the microscopic description of the process. Drying Technol. 2016. doi:10.1080/07373937.2015.1127933.

31. Iryani DA, Kumagai S, Nonaka M, Nagashima Y, Sasaki K, Hirajima T. The hot compressed water treatment of solid waste material from the sugar industry for valuable chemical production. Int J Green Energy. 2014;11:577–88.